Available online at www.sciencedirect.com
ScienceDirect
Journal of Photochemistry and Photobiology A: Chemistry 186 (2007) 254–262
Journal of Photochemistry and Photobiology A:Chemistry
www.elsevier.com/locate/jphotochem

# Surface photochemistry: Dibenzo-*p*-dioxin adsorbed onto silicalite, cellulose and silica

L.F. Vieira Ferreira [a,*], J.P. Da Silva [a,b], I. Ferreira Machado [a], T.J.F. Branco [a], J.C. Moreira [c]

[a] *Centro de Química-Física Molecular—Complexo Interdisciplinar, Instituto Superior Técnico, Av. Rovisco Pais, 1049-001 Lisboa, Portugal*
[b] *FCT, Universidade do Algarve, Campus de Gambelas, 8005-139 Faro, Portugal*
[c] *Centro de Estudos da Saúde do Trabalhador e Ecologia Humana, ENSP, Fundação Oswaldo Cruz, Rua Leopoldo Bulhões 1480, Rio de Janeiro, RJ 21041-210, Brazil*

Received 7 June 2006; received in revised form 27 July 2006; accepted 18 August 2006
Available online 30 August 2006

**Abstract**

Laser-induced luminescence of argon purged and air-equilibrated samples of dibenzo-*p*-dioxin adsorbed onto three different solid powdered supports, silicalite, cellulose and silica, revealed the existence of both fluorescence and phosphorescence emissions at room temperature.

A remarkable difference in transient absorption spectra was found when dibenzo-*p*-dioxin was included within the narrow internal channels of silicalite: triplet–triplet absorption of dibenzo-*p*-dioxin was detected in the silicalite case as a host, simultaneous with radical cation formation immediately after pulsed laser excitation (in the hundreds of nanoseconds time scale) while in the case of cellulose and silica as adsorbents, absorption transients arising from 2,2′-biphenylquinone and possibly from the spiroketone were found. For all hosts dibenzo-*p*-dioxin exhibits a transient band peaking at 330–340 nm in the microsecond and millisecond time scales, which we assigned to the biradical of dibenzo-*p*-dioxin.

Diffuse reflectance laser flash photolysis and chromatographic techniques provided complementary information, the former about transient species and the latter regarding the final products formed after laser irradiation at 266 nm. Product analysis and identification clearly show that the photodegradation products are dependent on the host, the photochemistry being much more rich and complex in the cellulose and silica cases, where the main detected photoproduts were 2,2′-dihydroxybiphenyl and 1-hydroxydibenzofuran. In the case of silicalite as host, which has a channel-like internal structure and reduced space available for the guest dioxin, photodegradation reactions are highly reduced or even inhibited and no photodegradation products were detected.


*Keywords:* Surface photochemistry; Dibenzo-*p*-dioxin; Silicalite; Cellulose; Silica; Diffuse reflectance; Flash photolysis; Laser-induced fluorescence; Room temperature phosphorescence; Lifetime distribution spreadsheet; Photodegradation products

## 1. Introduction

Dibenzo-*p*-dioxin (DBD) derivatives and related compounds, namely polychlorinated dioxins (PCDBDs) and dibenzofurans (PCDBFs) are carcinogenic compounds, which origin is predominantly anthropogenic, usually the combustion of chlorinated organic wastes [1–4]. These compounds are highly dangerous when introduced in the food webs, therefore a large interest exists in the study of the adsorption and photodegradation of these materials either in suitable hosts (with nanocavities of well-known dimensions and physical–chemical characteristics) [3,4], or simply in solution photodegradation studies [1] (Scheme 1).

Time-resolved laser-induced luminescence, diffuse reflectance laser flash-photolysis and ground state diffuse reflectance absorption spectroscopy are relatively new techniques that can be applied to study opaque and crystalline systems [5–9]. These solid-state photochemical methods have been recently applied by our group to study several organic compounds adsorbed onto different hosts such as *p-tert*-butylcalix[*n*]arenes (with

* Corresponding author. Tel.: +351 21 84 19 252; fax: +351 21 84 64 455.
*E-mail address:* LuisFilipeVF@ist.utl.pt (L.F.V. Ferreira).

1010-6030/$ – see front matter © 2006 Elsevier B.V. All rights reserved.
doi:10.1016/j.jphotochem.2006.08.015

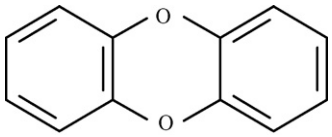

Scheme 1.

$n = 4$, 6 and 8) and derivatives [10], microcrystalline cellulose [11], silicalite and cyclodextrins [12], silica [13], resorcinarene frameworks [14], and reversed phase silicas [15], among others. Molecules such as benzophenone [10,11a,16], benzil [10c,14] and other ketones and thioketones [17] were used for probing these hosts.

Time-resolved diffuse reflectance absorption technique was also applied to the powdered solid samples of these compounds proving undoubtedly the inclusion of guest molecules within the cavities or internal channels of these hosts, and the existence of specific photodegradation pathways depending on the host [10,15]. In several cases the environment confinements play a decisive role in the photochemical behaviour of the adsorbed probe [15].

Silicalite is a de-aluminated analogue of ZSM-5 zeolites. The lack of substitutional aluminium results in silicalite having no catalytic or exchange properties, compared with the HZSM-5 zeolite [18]. Silicalite is the only known hydrophobic form of silica and is capable of adsorbing small organic molecules up to about 6 Å of kinetic diameter, even removing them from water [18,19]. Silicalite as a host provides a very rigid and in many cases constrained environment for the guest molecules, the internal cavities being near circular zig–zag channels (free-cross-section $5.4 \pm 0.2$ Å) which intersect the elliptical straight channels (free-cross-section 5.7–5.8 Å × 5.1–5.2 Å). Both channels are defined by 10-rings of oxygen ions [18]. Therefore, inclusion sites are non-homogeneous and three possible locations are predictable according to the silicalite structure described above: circular channels (the smaller ones), elliptical channels and the cross-points of these two, where probes may have more space available for emplacement [20].

It is of considerable importance to stress that isooctane (solvent used for sample preparation) does not penetrate into the silicalite or HZSM-5 channels due to stereo chemical restrictions (too big to penetrate) and also that for loadings of probe molecules greater than about 20 μmol/g of silicalite, the oxygen of the air is not able to penetrate into the internal structure of silicalite and no oxygen quenching effect exists and probes may exhibit room temperature phosphorescence.

Microcrystalline cellulose is a powdered solid support with the remarkable property of protecting adsorbed probes from oxygen action [5,11]. Adsorption of probes on microcrystalline cellulose can be achieved by the use of a solution of a probe with a polar protic (e.g. alcohols) or aprotic (e.g. acetonitrile, acetone, dioxane) solvents. When the solid substrate is added to this solution, cellulose to cellulose hydrogen bonds are replaced by cellulose to solvent bonds and the matrix exhibits a certain degree of swelling which depends on the solvent used for sample preparation [11]. Probes can then penetrate within the polymer chains and stay entrapped after solvent removal.

The 60 Å pore silica is also a solid powdered host where the silanol groups of the silica surface (≡Si–OH) play an important role in what regards surface-specific interactions with probes, as well as they create a polar environment to adsorbed molecules. Different adsorption sites of the silica gel surface exist (the 60 Å size reported for the pore average diameter means that the maximum of the distribution of the pore sizes is at 60 Å but, of course, larger and smaller pores exist, as is clearly indicated for several silicas gels in Ref. [21]), therefore resulting in different conformations for adsorbed molecules from which different luminescence emissions may exist from a single probe. This surface does not provide surface adsorbed probes a protection against oxygen quenching.

In this paper these three hosts for DBD were studied: silicalite, cellulose and 60 Å pore silica. A comparison of the photochemical behaviour of DBD was made, showing the occurrence of different photochemical reactions of DBD upon inclusion within the internal channels of silicalite, and on the surface of 60 Å pore silica or cellulose, resulting in the absence of photochemistry or in the formation of different new species which depend on the host surface characteristics.

## 2. Experimental

### 2.1. Materials

Dibenzo-*p*-dioxin was purchased from Cambridge Isotope Laboratories in the highest purity available and was used without further purification.

Silicalite (Union Carbide), 60 Å pore silica gel (Merck, 70–230 mesh), HZSM-5 (UOP Adsorbents, Si/Al = 19) and microcrystalline cellulose (Fluka DSO) were used as powdered solid supports as received after checking its purity by the use of ground state diffuse reflectance absorption spectroscopy. All solvents under use, hexane, dichloromethane, *iso*-octane, ethanol, methanol and acetonitrile were from Merck, Lichrosolv grade. 2,2′-Dihydroxybiphenyl and 2-hydroxydibenzofuran were from Aldrich. Water was deionised and distilled.

### 2.2. Sample preparation

The samples used in this work were prepared using the solvent evaporation method. This method consists in the addition of a solution containing the probe to the previously dried powdered solid substrate, followed by solvent evaporation from the stirred slurry in a fume cupboard. Hexane or dichloromethane were used for sample preparation for the 60 Å silica case because they evaporate easily at room temperature in the fume cupboard. In the case of the DBD/silicalite and DBD/HZSM-5 samples *iso*-octane was used for DBD inclusion into the channels of the adsorbents, because the solvent molecule is not able to penetrate into the channels due to its molecular dimensions. Microcrystalline cellulose samples were prepared by adding the probe solution after swelling this substrate with ethanol. The final solvent removal was performed overnight in an acrylic chamber with an electrically heated shelf (Heto, Model FD 1.0-110) with

temperature control (30 ± 1 °C) and under moderate vacuum at a pressure of *ca.* $10^{-3}$ Torr.

## 3. Methods

### 3.1. Ground state diffuse reflectance absorption spectra (GSDR)

Ground state absorption spectra for the solid samples were recorded using an OLIS 14 spectrophotometer with a diffuse reflectance attachment. Further details are given elsewhere [5,19a].

### 3.2. Laser-induced luminescence (LIL) and diffuse reflectance laser flash photolysis (DRLFP) systems

Schematic diagrams of the LIL and of the DRLFP systems are presented in Refs. [5,20]. Laser flash photolysis experiments were carried out with the fourth harmonic of a Nd:YAG laser (266 nm, *ca.* 6 ns FWHM, ∼10–30 mJ/pulse) from B.M. Industries (Thomson-CSF, model Saga 12-10), in the diffuse reflectance mode. The light arising from the irradiation of solid samples by the laser pulse is collected by a collimating beam probe coupled to an optical fiber (fused silica) and is detected by a gated intensified charge coupled device Oriel model Instaspec V (Andor ICCD, based on the Hamamatsu S57 69-0907). The ICCD is coupled to a fixed imaging compact spectrograph (Oriel, model FICS 77441). The system can be used either by capturing all light emitted by the sample or in a time-resolved mode by using a delay box (Stanford Research Systems, model D6535). The ICCD has high speed gating electronics (2.2 ns) and intensifier and covers the 200–900 nm wavelength range. Time-resolved absorption and emission spectra are available in the nanosecond to second time range. Transient absorption data are reported as percentage of absorption (%Abs.), defined as $100\Delta J_t/J_o = (1 - J_t/J_o)100$, where $J_o$ and $J_t$ are diffuse reflected light from sample before exposure to the exciting laser pulse and at time $t$ after excitation, respectively. For laser-induced luminescence experiments either a Nd:YAG laser (266 nm excitation) or a $N_2$ laser (PTI model 2000, *ca.* 600 ps FWHM, ∼1.1 mJ per pulse), were available to be used. In this latter case the excitation wavelength is 337 nm. With these set-ups, both fluorescence and phosphorescence spectra are easily available (by the use of the variable time gate width and start delay facilities of the ICCD).

### 3.3. Irradiation and product analysis

Photodegradation studies under lamp irradiation were conducted in a reactor previously used to study the photochemistry of several compounds at the solid/gas interface [10a,c,12b,15–17]. The lamp irradiation was performed at 254 nm using a 16 W low-pressure mercury lamp (Applied Photophysics) without filters and without refrigeration. The samples were irradiated in a quartz cell placed at 1 cm from the lamp surface, in air-equilibrated conditions, during 3.5 h. Laser irradiation at 266 nm, in argon atmosphere, was also performed. In this case the samples were irradiated in a quartz cell during 0.5 h at five pulses (30 mJ) per second. The samples were mixed every 5 min during the laser irradiation process. Non-irradiated and irradiated samples were analysed after extraction with methanol (a known weight of sample in a known volume of solvent) followed by centrifugation. Photolysis was followed by HPLC using a Merck-Hitachi 655A-11 chromatograph equipped with detectors 655A-22 UV and Shimadzu SPD-M6A Photodiode Array. A column LiChroCART 125 (RP-18, 5 μm) Merck was used and the runs were performed using mixtures of water/acetonitrile. The extracts were also analysed by GC–MS using a Hewlett Packard 5890 Series II gas chromatograph with a 5971 series mass selective detector (E.I. 70 eV). A Restek RTX-20 capillary column with 20 m and 0.18 mm i.d. was used. The initial temperature 70 °C was maintained during 5 min and then a rate of 5 °C/min was used until 250 °C.

## 4. Results and discussion

### 4.1. Ground state diffuse reflectance absorption spectra

Ground state diffuse reflectance absorption spectra for DBD adsorbed onto silicalite, microcrystalline cellulose and 60 Å pore silica, were obtained with the use of an integrating sphere [5,11], and also with the use of our diffuse reflectance laser flash photolysis set-up, by triggering the system in the normal way [5], and recording the lamp profile (without laser excitation) for the guest–host sample and also for the host alone.

This latter procedure has the advantage of excluding the sample's luminescence (if it exists) because of the use of the analysing fixed monochromator which is coupled to the ICCD [5]. A 450 W xenon lamp was used, therefore promoting photochemistry to occur in the sample under study, even without the laser use. The results obtained with the two set-ups are fully compatible, but of course more photodegradation products were formed (during the time needed to record each spectrum) in the case of the diffuse reflectance laser flash photolysis set-up. These latter data are presented in Fig. 1.

DBD ground state absorption $S_o \rightarrow S_1$ transition ($\pi \rightarrow \pi^*$) has absorption maxima at about 298, 303 and 306 nm for the three hosts, respectively (Fig. 1). The solution spectra of DBD (in cyclohexane) also presents this $\pi \rightarrow \pi^*$ transition in the UV peaking at approximately 290 nm [2]. The bathochromic shift results from the interaction of DBD with the solid surfaces and also reflects the increase of the polarity felt by the guest molecule going from silicalite to cellulose and to silica. Also some broadening effect of this band in the same order exists and this is probably related to heterogeneity of the adsorbent surface.

Within silicalite DBD is included into the rigid channel type structure of this adsorbent, while in cellulose stays entrapped into the natural polymer chains (ethanol was used as solvent for sample preparation as in Ref. [11]). Finally for silica as adsorbent DBD molecules are simply onto the silica surface. These adsorbent characteristics (in what regards entrapment) deeply affect the ground state absorption spectra presented in Fig. 1. When DBD is rigidly included into the narrow channels of silicalite no new photochemically generated products were detected and diffuse reflectance spectra are very similar to the ones obtained

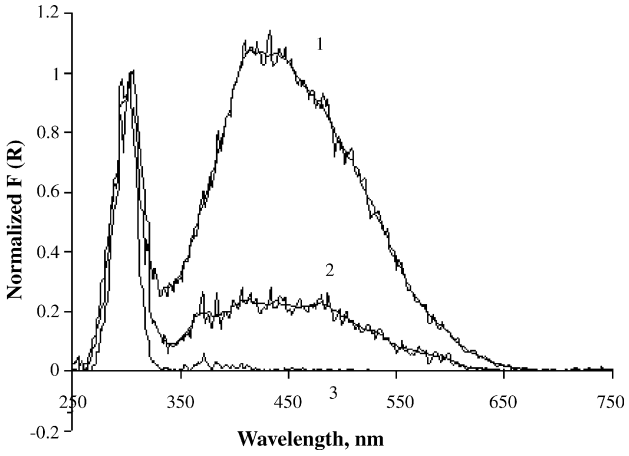


Fig. 1. Diffuse reflectance ground state absorption of previously non-irradiated samples of DBD adsorbed on 60 Å silica (curve 1), microcrystalline cellulose (curve 2) and silicalite (3). The concentration is 100 μmol $g^{-1}$ in all cases. All curves are normalized at the maximum absorption (higher energy) of DBD. All spectra were obtained with the DRLFP set-up as described in the text.

in cyclohexane. However, for the silica surface case, were DBD experiences much more freedom when adsorbed onto the host surface, strong photochemistry exists, and new bands peaking at about 420 nm and 530 nm were detected. In the case of cellulose the spectrum resembles the silica surface one, although the new formed products are present in smaller amounts.

From previously published work from Thomas and co-workers [2] and Wan et al. [1], we know that the ~530 nm band corresponds to the 2,2′-biphenylquinone absorption [1,2] while the ~420 nm band absorption was tentatively assigned to the spiroketone absorption [1a].

In curve 1 of Fig. 1 (DBD adsorbed on 60 Å pore silica), the 354 nm absorption band of the biphenylquinone [1a] is not observed, probably because it is masked by the broadening effect in the absorption spectra of the spiroketone and the biphenylquinone on the surface, due to distortions of the molecule induced by the heterogeneity of the surface.

### *4.2. Room temperature and 77 K laser-induced luminescence*

Fig. 2a presents the room temperature luminescence solution spectra of DBD in methanol (argon purged sample, O.D. = 2 at 266 nm) while Fig. 2b exhibits the 77 K time-resolved fluorescence spectra of the same sample, in a nanosecond time scale. Fig. 2c refers to the phosphorescence emission spectra at 77 K of the same sample with the use of a millisecond time scale. All these time-resolved emission spectra were obtained by the use of our ICCD which has time gate capabilities, enabling us to separate prompt luminescence following laser pulse (fluorescence) from longer lived emissions (phosphorescence).

Time-resolved emission spectra in solution and at room temperature were also obtained under air-equilibrated conditions and were identical in shape to the ones obtained with argon purged samples but about 200 times less intense. The important features to take into account from Fig. 2a are the detection of an emission peaking at about 340 nm and a much stronger one peaking at about 392 nm with shoulders at 374 nm and 416 nm. Half-lives of about 25 ns and 130 ns were determined for these two emissions which we assign to the room temperature fluorescence and room temperature phosphorescence of DBD in methanol solution, in accordance with the work of Thomas and co-workers [2] for DBD on a laponite surface, based on the band positions.

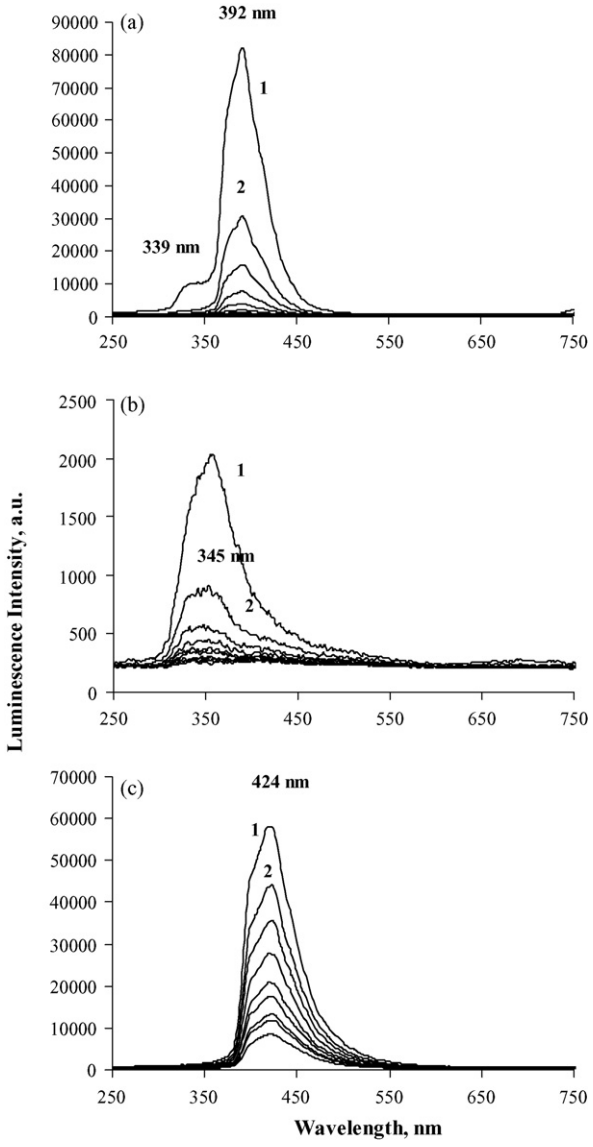


Fig. 2. Time-resolved luminescence of argon purged samples of DBD in methanol (the excitation wavelength was 266 nm at 30 mJ/pulse, O.D. ~2). (a) Room temperature emission spectra (fluorescence and phosphorescence) in a ns time scale; curve 1, 0 ns after laser pulse and step = 100 ns. (b) 77 K fluorescence emission spectra in a ns time scale; curve 1, 0 ns after laser pulse and step = 50 ns. (c) 77 K phosphorescence emission spectra in a ms time scale; curve 1, 200 μs after laser pulse and step = 1.5 ms.

The phosphorescence spectra of DBD in EPA matrix at 77 K was reported previously by Pohland et al. [22], and the room temperature fluorescence (RTF) of DBD in hexane, and room temperature phosphorescence (RTP) or low temperature phosphorescence (LTP) of DBD spotted onto filter paper were obtained by Winefordner et al. [23], by the use of steady-state emission techniques.

The use of laser-induced fluorescence and phosphorescence techniques, with a laser as pulsed excitation source (266 nm excitation with about 6–7 ns halfwidth), and the simultaneous use of time-gated detectors (ICCD detection), enabled us the detection of some interesting features we will describe now: We emphasize that the low temperature fluorescence emission (77 K) also peaks at about 345 nm but the half-life is now *ca.* 60 ns (Fig. 2b) while at room temperature it was shorter. This is a normal effect; sample rigidity reduces the non-radiative pathways of deactivation and the singlet state excited species lives longer. In what regards the 77 K phosphorescence emission (Fig. 2c) the spectra is similar to the one obtained at RT, but a clear bathochromic deviation was detected (about 25 nm).

The planarity or folded conformations of DBD in the ground and excited states has been the subject of a certain controversy, either in recent [24,25] or less recent publications [26,27]. A dipole moment of 0.55 D was measured in benzene solutions [27], indicating a folded ground state conformation (angle of folding about 165° [26,27]), while X-ray studies of DBD crystals indicate planar conformation within experimental error [26]. DBD structure is markedly non-rigid in solution due to a very low barrier to a butterfly flapping motion.

Spectra presented in Fig. 2a (methanol solution, RT) exhibit a phosphorescence maximum at about 395 nm, corresponding to a relatively fast emission from a folded conformation, while spectra in Fig. 2c correspond to much more long-lived species due to the low temperature (77 K) and DBD has time enough to assume a planar conformation because the excited triplet state lives now milliseconds. The *ca.* 25 nm bathochromic shift results from the planar conformation assumed by DBD in T1. Both fluorescence emissions are relatively fast and the molecule has no time to assume relaxed excited state planar conformation, therefore the fluorescence maximum is relatively insensitive to the lowering of temperature. The planar conformation of DBD in the triplet state provides an energy stabilization, which results in the observed bathochromic shift possibly by increased electron density delocalization.

Fig. 3a presents the room temperature luminescence spectra for powdered samples of DBD included into silicalite narrow channels, Fig. 3b refers to DBD entrapped within microcrystalline polymer chains and finally Fig. 3c shows DBD emissions when adsorbed onto 60 Å pore silica. All samples were air equilibrated.

The relative importance of the fluorescence versus phosphorescence emissions varies in the three different substrates, and this is compatible with different conformations of the differently adsorbed molecules. In all cases the fluorescence emission decay is faster than the phosphorescence emission, the former always peaking around 340 nm and the latter peaking at about 395 nm, although bathochromic shifts with the increase of polarity going from silicalite to microcrystalline cellulose and silica can be observed, consistent with the $\pi$–$\pi^*$ nature of the emissive state. It is also interesting to note that in the microcrystalline cellulose and silica cases as substrates, the luminescence intensity is larger than in the case of the narrow channels of silicalite. This could seem unexpected, but when we take into account the fact that very fast radical cation and efficient biradical formation

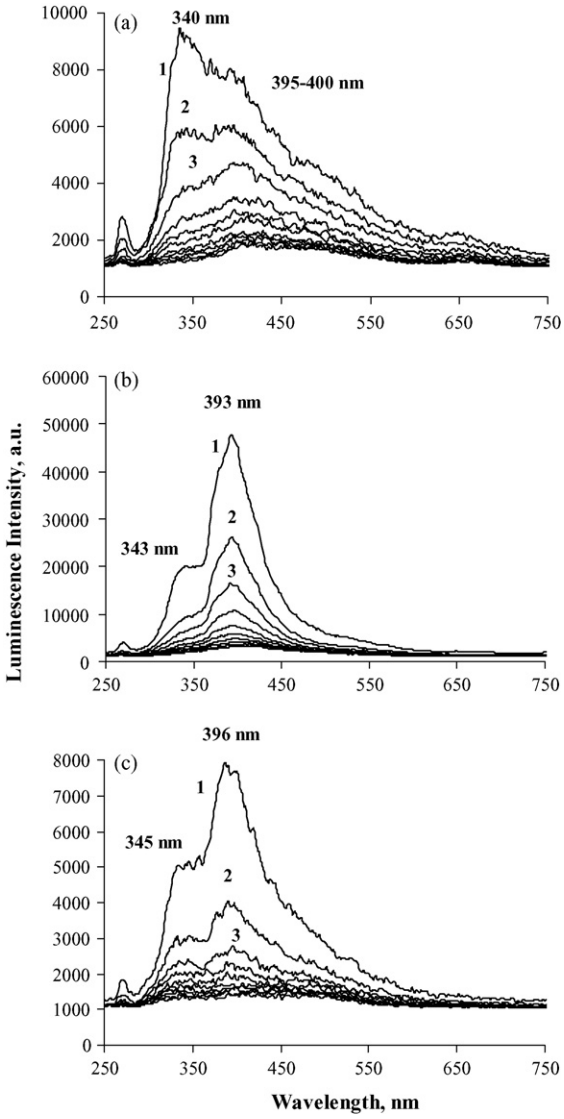


Fig. 3. Room temperature, time-resolved luminescence spectra of air-equilibrated samples of DBD on three different surfaces (the excitation wavelength was 266 nm at 30 mJ/pulse, 20 μmol $g^{-1}$). (a) Silicalite; curve 1, 0 ns after laser pulse and step = 100 ns. (b) Microcrystalline cellulose; curve 1, 0 ns after laser pulse and step = 100 ns. (c) 60 Å pore silica; curve 1, 0 ns after laser pulse and step = 50 ns.

occurs in this case, as will be shown in the diffuse reflectance transient studies section, this observation becomes quite reasonable.

A lifetime emission distribution study for the case of DBD entrapped within microcrystalline cellulose polymer chains is presented in Fig. 4, performed as described in a recent publication from our group [20]. Only one emissive species of DBD was detected with a narrow distribution of lifetimes peaking at 26 ns (with values at half maximum of 21 ns and 33 ns), the room temperature fluorescence of DBD. Another narrow distribution corresponding to the phosphorescence of DBD was seen, now with a lifetime of 216 ns (with values at half maximum of 199 ns and 235 ns). Both emissions are superimposed on a very large distribution with about 24 ns width at half maximum (from 0.5 ns to 24.3 ns), which arises from the absorbent, cellu-

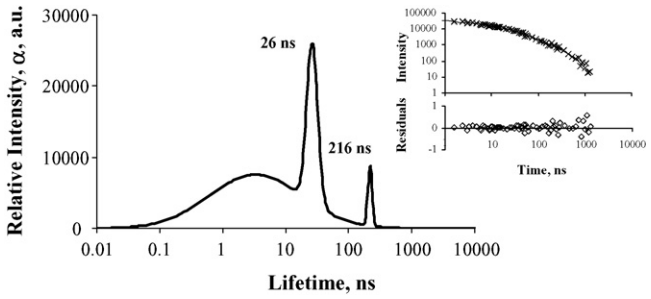


Fig. 4. Lifetime distributions for DBD onto cellulose recovered from time-resolved luminescence decays observed at 363 nm. The insets show the fitting of the recovered decay to the experimental data and also relative residuals.

lose (the substrate alone exhibits a similar lifetime distribution of the prompt emission, following 266 nm excitation, data not shown).

The lifetime distribution analysis was performed at a specific wavelength of analysis (363 nm) where both fluorescence and phosphorescence emissions exist. Therefore relative intensities of the lifetime distributions reflect the ratio of these two emissions at a specific wavelength and do not reflect the relative ratios of phosphorescence to fluorescence emissions.

### 4.3. Diffuse reflectance laser flash photolysis

Time-resolved absorption spectra of samples of DBD within the silicalite channels, entrapped within microcrystalline polymer and adsorbed onto 60 Å pore silica (Fig. 5a–c, respectively), were obtained by the use of diffuse reflectance laser flash photolysis technique, developed by Wilkinson et al. [6]. In this study the use of an intensified charged coupled device as detector allowed us to obtain time-resolved absorption spectra with nanometer spectral spacing [5].

All time-resolved spectra were obtained for air-equilibrated samples, exciting at 266 nm. Argon purged and oxygen saturated samples were also used to clarify the role of the triplet state of DBD in the photodegradation pathway.

Diffuse reflectance laser flash photolysis for DBD adsorbed onto the three surfaces under study provided us experimental information confirming the pathways for photodegradation identical to the ones described for aqueous and organic solutions [1], *i.e.* the case of cellulose and silica surfaces, but it also provided us relevant information on the photodegradation pathway in a constrained environment, *i.e.* silicalite, which is quite different from the one occurring in the case of the two other solid powdered supports.

In the case of the silicalite surface (Fig. 5a), a band peaking at about 330–340 nm is predominant in the spectra after 1 μs, and decays in the micro and millisecond time ranges. Immediately after the laser pulse (0 μs) a band peaking at 680 nm can be easily identified as the radical cation of DBD [2]. This surface has Lewis acid sites which act as electron acceptors and this process is instantaneous in the time scale of our experiments. If we take into account that this process it is not affected by the presence of oxygen either in air-equilibrated samples or in oxygen-purged samples it probably starts in the excited singlet

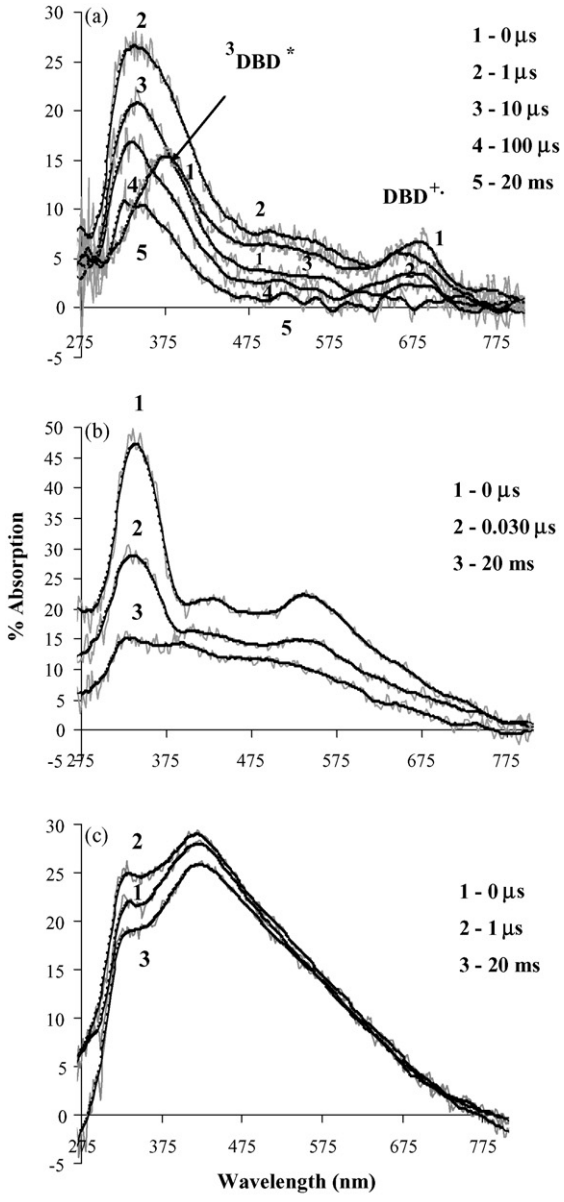


Fig. 5. Transient absorption spectra of DBD air-equilibrated samples of DBD on three different surfaces (the excitation wavelength was 266 nm at 30 mJ/pulse, 100 μmol g$^{-1}$). (a) Silicalite; (b) microcrystalline cellulose; (c) 60 Å pore silica.

state of DBD. Similar results regarding the formation of the radical cation of DBD were obtained with HZSM-5, which also contains Lewis acid sites.

Is DBD physical adsorbed and radical cation formation occurs or chemical adsorption exists and radical formation occurs? Literature (please see Refs. [2,20,21] therein) clearly points to the first hypothesis, namely because the radical cation was also generated by chemical methods and identification is simple. Also the transient peaking at 680 nm decays in less than 20 ms, as Fig. 5 shows. Anyway, after pumping the sample for about 36 h at elevated temperatures, we recorded the transient absorption spectra before and after the sample treatment, and the result was the disappearance of the dioxin, *i.e.* DBD is physical

adsorbed into silicalite channels, therefore the 680 nm band is from the radical cation of DBD.

Another very important transient absorption band is indicated in Fig. 5a, peaking at about 370 nm at time zero after the laser pulse. This band disappears in the hundreds of nanoseconds time range, and its decay occurs concomitantly with the phosphorescence of DBD in this media. Therefore, we assign this species to the triplet–triplet absorption of DBD. Silicalite narrow channels prevent the diffusion of oxygen molecules for probe loadings of 20 μmol $g^{-1}$ or higher, as reported by us in previous papers [12a,19], therefore preventing the quenching of the triplet state of DBD.

The 330–340 nm transient absorption is also not influenced by the presence of oxygen and, as we said, lives in the micro and millisecond time scales, this fact being valid also for cellulose (Fig. 5b) and silica surfaces (Fig. 5c). We believe the 330–340 nm band is neither the spiroketone (max. at about 420 nm [1]) nor the biphenylquinone [1,2] (max. at about 530 nm), which exit both in the cellulose and silica cases. Therefore we assign this band as the transient absorption of the biradical of DBD, formed in all surfaces under study via $^{1}DBD^{*}$.

The triplet–triplet absorption of DBD when adsorbed onto cellulose and silica is masked by the huge absorptions of the biradical, the spiroketone and the biphenylquinone.

The reason that it does not give rise to the spiroketone and the biphenylquinone in the silicalite case (as it does onto cellulose or silica, in a way as it does in solution [1]), is related to the steric hindrance imposed by the narrow dimensions of silicalite internal channels. The excited $^{1}DBD^{*}$ has no space enough to form neither the spiroketone nor the biphenylketone as the transient absorption spectra of Fig. 5a, in comparison with Fig. 5b and c clearly show.

From these data we could anticipate a reduced photochemistry of DBD included within the narrow channels of silicalite, and an opposite behaviour of DBD adsorbed onto cellulose or silica, and we will see in the next section (photodegradation studies) that this really is the case. Silicalite could influence the degradation pathways, in this case by imposing a restriction in the available intermediates as shown in Fig. 7.

### 4.4. Photodegradation products studies

The lamp and laser irradiated powdered samples of DBD were washed with methanol and extract analysed both by HPLC and GC–MS. The photoproduct distribution obtained after lamp and laser irradiations was similar, suggesting that biphotonic processes, if present, represent a minor degradation pathway in what regards the formation of the final photoproducts.

Fig. 6 presents the HPLC chromatograms of extracts of non-irradiated and irradiated samples (in the same conditions) of DBD on the three solid supports. The photoproduct distributions clearly indicate that DBD is stable in silicalite and that reactivity increases in the case of cellulose and is even higher in the silica's case. This result is in agreement with the ground state absorption spectra which show higher formation of photoproducts on silica than on cellulose and only probe absorption in the silicalite case. It is also consistent with the diffuse reflectance transient absorption data shown in Fig. 5.

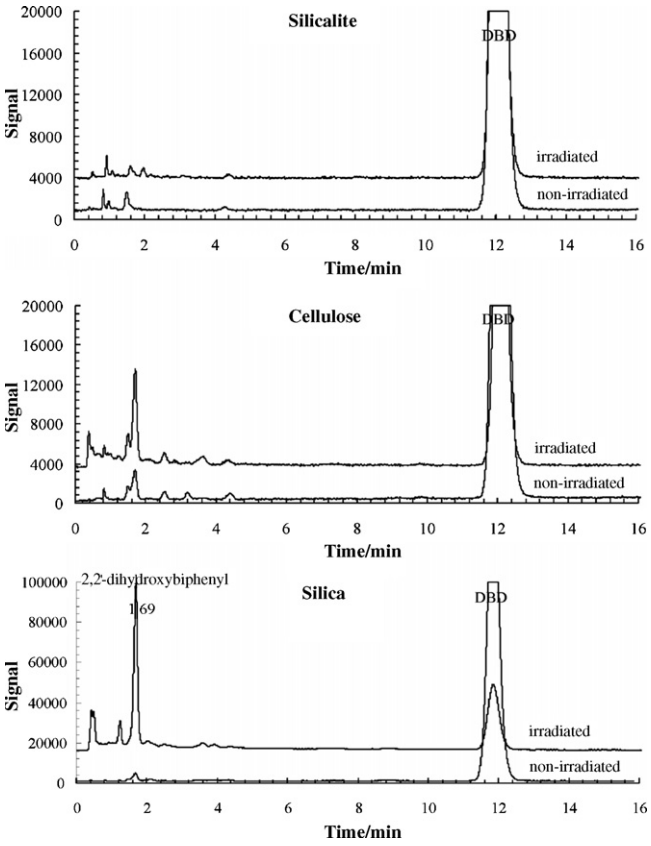


Fig. 6. HPLC chromatograms of the extracts of irradiated samples of DBD on the studied solid supports.

The main photoproduct is 2,2′-dihydroxybiphenyl. The identification was based on the analysis of an authentic sample. No absorption was detected at 420 nm or at 530 nm, assignable to the spiroketone [1a] and 2,2′-biphenylquinone [1,2], respectively, when the extracts were analysed using a diode array detector. The ground state absorption spectra of the irradiated solid samples are different from those of the corresponding extracts, indicating that chemical modification occurred upon extraction and analysis. Both biphenylquinone and spiroketone undergo chemical reactions in the dark indicating that these compounds do not survive to the extraction and analysis processes. The formation of 2,2′-dihydroxybiphenyl is in agreement with these results since the spiroketone leads to the biphenylquinone and this compound can form the main detected photodegradation product after hydrogen abstraction (see Fig. 7) [1].

A compound with mass spectrum compatible with 1-hydroxydibenzofurane was also detected but its formation is a minor degradation pathway.

Fig. 7 presents the reaction mechanism which includes all findings presented until now, and we stress that in the silicalite case, in spite of the detection of the presence of DBD radical cation and $^{3}DBD^{*}$, no relevant photochemistry occurs inside the narrow channels of this hydrophobic material. On the contrary,

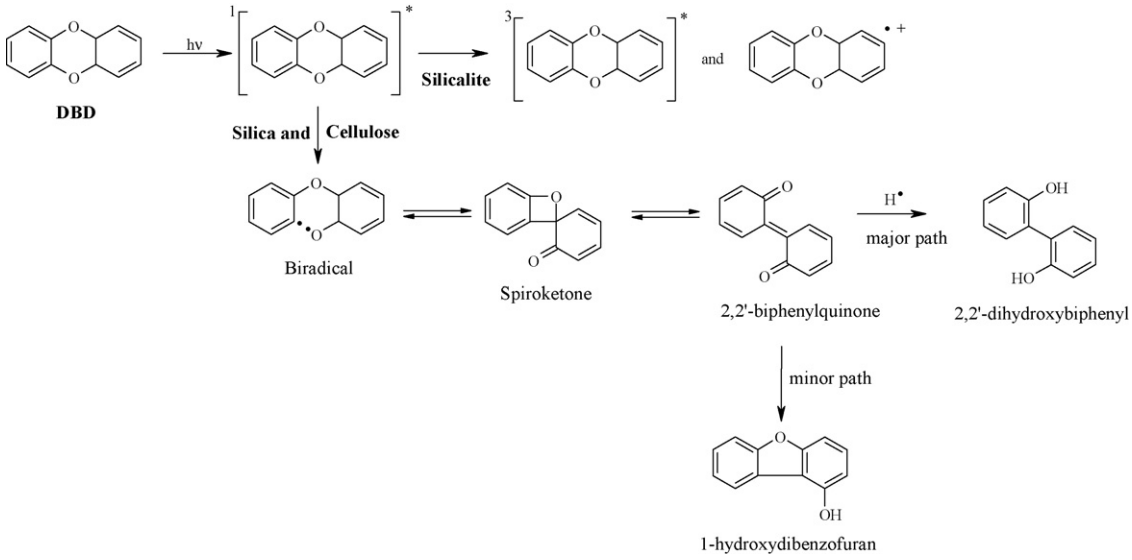


Fig. 7. Reaction mechanism for DBD photodegradation on surfaces of silicalite, cellulose and 60 Å silica.

when the adsorbents were cellulose and silica, a rich photochemistry exists, and the detected photoproducts were the same as in previous solution studies [1].

## 5. Conclusions

DBD exhibits fluorescence peaking at about 340 nm and also strong phosphorescence emission centred at about 395 nm in degassed solutions at room temperature while at 77 K the phosphorescence peaks at about 420 nm. The existence of folded and planar conformations explains this emission's behaviour. Fluorescence and phosphorescence emissions were also detected for DBD absorbed onto the three solid powdered supports under study.

The photochemistry of DBD adsorbed onto solid powdered surfaces strongly depends on the solid support characteristics. DBD degrades onto silica and cellulose during the ground state absorption studies, a behaviour similar to the one reported for methanol or acetonitrile solutions at room temperature where a strong and broad absorption band is formed between 350 and 600 nm [1a].

However, when adsorbed into the narrow channels of the hydrophobic zeolite, silicalite, DBD is remarkably stable, in spite of the fact that the $^3DBD^*$ was detected and lives less than 1 μs and also of the fact that long-lived transient absorptions of the radical cation of DBD and also DBD biradical were detected in the microsecond and millisecond time scales. These transient species regenerate ground state DBD and no significative amounts of photodegradation products were detected both by HPLC and GC–MS studies.

Based on the behaviour of the transient absorption bands in argon and $O_2$ saturated atmospheres, and on time-resolved luminescence results, the band centred at 370 nm was assigned to the triplet–triplet absorption of DBD. The transient absorption band peaking at 330–340 nm was assigned to the biradical transient absorption of DBD.

DBD radical cation transient absorption was detected only onto silicalite or HZSM-5. The broad absorption band observed in silica and cellulose ground state absorption studies was also observed in flash photolysis experiments. According to literature, this band corresponds to the transient absorption of the spiroketone (at about 420 nm) and to the 2,2′-biphenylquinone (at about 530 nm) [1a].

The main degradation product detected for silica and cellulose adsorption after extraction with methanol was 2,2′-dihydroxybiphenyl. 1-Hydroxybibenzofuran was also detected, but as a minor photodegradation product.

## Acknowledgements

JPS thanks FCT for a Post-Doctoral fellowship SFRH/BPD/15589/2001, TJFB thanks FCT for a PhD grant SFRH/BD/8143/2002 and IFM thanks FSE for financial support.

## References

[1] (a) S. Rayne, R. Sasaki, P. Wan, Photochem. Photobiol. Sci. 4 (2005) 876–886;
(b) B. Guan, P. Wan, J. Photochem. Photobiol. A: Chem. 80 (1994) 199–210;
(c) B. Guan, P. Wan, J. Chem. Soc., Chem. Commun. (1993) 409–410.
[2] Y. Mao, S. Pankassem, J.K. Thomas, Langmuir 9 (1993) 1504–1512.
[3] R. Jager, A.M. Schneider, P. Behrens, B. Henkelmann, K.-W. Schramm, Chem. Eur. J. 10 (2004) 247–256.
[4] Y. Guan, Y. Liu, W. Wu, K. Sun, Y. Li, P. Ying, Z. Feng, C. Li, Langmuir 21 (2005) 3877–3880.
[5] A.M. Botelho do Rego, L.F. Vieira Ferreira, in: H.S. Nalwa (Ed.), Handbook of Surfaces and Interfaces of Materials, vol.2, Academic Press, 2001, pp. 275–313, Chapter 7.
[6] (a) F. Wilkinson, G.P. Kelly, in: M. Anpo, T. Matsuara (Eds.), Photochemistry on Solid Surfaces, Elsevier, Amsterdam, 1989, pp. 31–47;
(b) F. Wilkinson, G.P. Kelly, in: J.C. Scaiano (Ed.), Handbook of Organic Photochemistry, vol. 1, CRC Press, Boca Raton, 1989, pp. 293–314, Chapter 12;
(c) F. Wilkinson, C.J. Willsher, Chem. Phys. Lett. 104 (1984) 272–276.
[7] J.C. Scaiano, H. Garcia, Acc. Chem. Res. 32 (1999) 783–793.

[8] S. Hashimoto, J. Photochem. Photobiol. C: Photochem. Rev. 4 (2003) 19–49.
[9] (a) J.K. Thomas, Chem. Rev. 105 (2005) 1683–1734;
(b) J.K. Thomas, Photochem. Photobiol. Sci. 3 (2004) 483–488.
[10] (a) L.F. Vieira Ferreira, M.R. Vieira Ferreira, J.P. Da Silva, I. Ferreira Machado, A.S. Oliveira, J.V. Prata, Photochem. Photobiol. Sci. 2 (2003) 1002–1010;
(b) L.F. Vieira Ferreira, M.R. Vieira Ferreira, A.S. Oliveira, T.J.F. Branco, J.V. Prata, J.C. Moreira, Phys. Chem. Chem. Phys. 4 (2002) 204–210;
(c) L.F. Vieira Ferreira, I. Ferreira Machado, A.S. Oliveira, M.R. Vieira Ferreira, J.P. Da Silva, J.C. Moreira, J. Phys. Chem. B 106 (2002) 12584–12593.
[11] (a) L.F. Vieira Ferreira, J.C. Netto-Ferreira, I. Khmelinskii, A.R. Garcia, S.M.B. Costa, Langmuir 11 (1995) 231–236;
(b) L.F. Vieira Ferreira, M.R. Freixo, A.R. Garcia, F. Wilkinson, J. Chem. Soc. Faraday Trans. 88 (1992) 15–22;
(c) L.F. Vieira Ferreira, A.R. Garcia, M.R. Freixo, S.M.B. Costa, J. Chem. Soc. Faraday Trans. 89 (1993) 1937–1944.
[12] (a) L.F. Vieira Ferreira, M.R. Vieira Ferreira, A.S. Oliveira, J.C. Moreira, J. Photochem. Photobiol. A: Chem. 153 (2002) 11–18;
(b) J.P. Da Silva, L.F. Vieira Ferreira, A.M. Da Silva, A.S. Oliveira, J. Photochem. Photobiol. A: Chem. 151 (2002) 157–164.
[13] L.F. Vieira Ferreira, M.J. Lemos, M.J. Reis, A.M. Botelho do Rego, Langmuir 16 (2000) 5673–5680.
[14] B.Q. Ma, L.F. Vieira Ferreira, P. Coppens, Org. Lett. 6 (2004) 1087–1090.
[15] L.F. Vieira Ferreira, I. Ferreira Machado, J.P. Da Silva, T.J.F. Branco, Photochem. Photobiol. Sci. 5 (2006) 665–673.
[16] (a) J.P. Da Silva, I. Ferreira Machado, J.P. Lourenço, L.F. Vieira Ferreira, Micropor. Mesopor. Mater. 84 (2005) 1–10;
(b) J.P. Da Silva, I. Ferreira Machado, J.P. Lourenco, L.F. Vieira Ferreira, Micropor. Mesopor. Mater. 89 (2006) 143–149.
[17] L.F. Vieira Ferreira, I. Ferreira Machado, A.S. Oliveira, J.P. Da Silva, A. Krawczyk, M. Sikorski, J. Mol. Struct., in press.
[18] (a) E.C. Flaningen, J.M. Bennet, R.W. Grose, R.L. Patton, R.M. Kirchner, J.V. Smith, Nature 271 (1978) 512–516;
(b) G.M.W. Shultz-Sibbel, D.T. Gjerde, C.D. Chriswell, J.S. Fritz, W.E. Colleman, Talanta 29 (1982) 447–452;
(c) D.M. Bibby, N.B. Millestone, L.P. Aldridge, Nature 280 (1979) 664–665.
[19] (a) L.F. Vieira Ferreira, A.S. Oliveira, J.C. Netto-Ferreira, in: A. Kotyk (Ed.), Fluorescence Microscopy and Fluorescence Probes, vol. 3, Espero Publishing, Prague, 1999, pp. 199–208;
(b) L.F. Vieira Ferreira, J.C. Netto-Ferreira, S.M.B. Costa, Spectrochim. Acta A 51 (1995) 1385–1388.
[20] T.J.F. Branco, A.M. Botelho do Rego, I. Ferreira Machado, L.F. Vieira Ferreira, J. Phys. Chem. B 109 (2005) 15958–15967.
[21] N.J. Turro, Tetrahedron 43 (1987) 1589–1616.
[22] A.E. Pohland, G.C. Yang, J. Agric. Food Chem. 20 (1972) 1093–1099.
[23] I.M. Khasawneh, J.D. Winefordner, Talanta 35 (1988) 267–270.
[24] I. Ljubic, A. Sabljic, J. Phys. Chem. A 109 (2005) 8209–8217.
[25] E.A. Gastilovich, V.G. Klimenko, N.V. Korol'kova, R.N. Nurmukhametov, Chem. Phys. 182 (2002) 265–275.
[26] G. Fronza, E. Ragg, J. Chem. Soc.: Perkin Trans. II (1982) 291–293.
[27] F.P. Colonna, G. Distefano, V. Galasso, K.J. Irgolic, C.E. King, G.C. Pappalardo, J. Organomet. Chem. 146 (1978) 235–244.